

On the effect of the ionising background on the Ly α forest autocorrelation function

Satya Gontcho A Gontcho¹, Jordi Miralda-Escudé^{1,2}, Nicolás G. Busca^{3,4,5}

¹*Institut de Ciències del Cosmos, Universitat de Barcelona/IEEC, Barcelona 08028, Catalonia, Spain*

²*Institució Catalana de Recerca i Estudis Avançats, Barcelona, Catalonia, Spain*

³*APC, Université Paris Diderot-Paris 7, CNRS/IN2P3, 10 rue A. Domon & L. Duquet, Paris, France*

⁴*Observatório Nacional, Rua Gal. José Cristino 77, Rio de Janeiro, RJ - 20921-400, Brazil*

⁵*Laboratório Interinstitucional de e-Astronomia, - LIneA, Rua Gal. José Cristino 77, Rio de Janeiro, RJ - 20921-400, Brazil*

Accepted 2014 April 29 ; Received 2014 April 22; in original form 2014 February 5

ABSTRACT

An analytical framework is presented to understand the effects of a fluctuating intensity of the cosmic ionising background on the correlations of the Ly α forest transmission fraction measured in quasar spectra. In the absence of intensity fluctuations, the Ly α power spectrum should have the expected cold dark matter power spectrum with redshift distortions in the linear regime, with a bias factor b_δ and a redshift distortion parameter β that depend on redshift but are independent of scale. The intensity fluctuations introduce a scale dependence in both b_δ and β , but keeping their product $b_\delta\beta$ fixed. Observations of the Ly α correlations and cross-correlations with radiation sources like those being done at present in the BOSS survey of SDSS-III (Busca et al. 2013; Slosar et al. 2013; Font-Ribera et al. 2014) have the potential to measure this scale dependence, which reflects the biasing properties of the sources and absorbers of the ionising background. We also compute a second term affecting the Ly α spectrum, due to shot noise in the sources of radiation. This term is very large if luminous quasars are assumed to produce the ionising background and to emit isotropically with a constant luminosity, but should be reduced by a contribution from galaxies, and by the finite lifetime and anisotropic emission of quasars.

Key words: Lyman α Forest – intergalactic medium – diffuse radiation – cosmology – quasar – quasar: luminosity function.

1 INTRODUCTION

The Ly α forest absorption measured in spectra of high-redshift quasars has now been established as a powerful tracer of large-scale structure. Assuming that the intrinsic continuum spectrum of the observed quasar can be accurately modelled, then the observed flux divided by the fitted continuum yields the transmitted fraction, $F = e^{-\tau}$ (where τ is the optical depth), at every wavelength pixel. This one-dimensional map that is obtained from the spectrum of every observed source is related (neglecting the contamination by metal lines) to the gas density, temperature and peculiar veloc-

ity of the hydrogen gas in the intergalactic medium that is intercepted by the line of sight.

After the initial measurements of the Ly α power spectrum along the line of sight from individual spectra (Croft et al. 1998, 1999; McDonald et al. 2000; Croft et al. 2002; McDonald et al. 2006), the first determination of the power spectrum of the Ly α forest in three-dimensional redshift space came with the BOSS survey of SDSS-III (Eisenstein et al. 2011; Dawson et al. 2013). Analysis of the first 14000 quasars led to the detection of redshift space distortions (Slosar et al. 2011), as expected in a simple biased linear theory where the Ly α power spectrum follows that of the dark matter with two

bias parameters, reflecting the large-scale variation of the mean Ly α transmission with the fluctuation in the mean mass density and peculiar velocity gradient.

However, large-scale fluctuations in the Ly α forest can also be affected by variations in the intensity of the ionising background radiation, as well as the imprint that reionisation may have left on the gas temperature distribution as a function of gas density. These effects have been studied and discussed by several authors in the past. Analytic models of randomly distributed sources were considered by Zuo (1992), and numerical realizations of random sources to compute the fluctuation properties of the ionising background were used in several subsequent papers (Croft et al. 1999; Croft 2004; Meiksin & White 2004; McDonald et al. 2005; Slosar et al. 2009; White et al. 2010). The impact of these ionising background fluctuations on the Ly α forest were found to be generally small compared to the intrinsic Ly α forest fluctuations due to the large-scale structure of the mass distribution. However, as pointed out in the early work of Croft et al. (1999), the long mean free path of ionising radiation in the intergalactic medium at $z \sim 3$ implies that the fluctuations induced by the ionising background can become relatively more important in the limit of very large scales. These large scales are now becoming highly relevant with the recent detections of the BAO peak in the Ly α forest (Busca et al. 2013; Slosar et al. 2013; Font-Ribera et al. 2014; Delubac et al. 2014).

In this paper we reanalyse with an analytic method the impact of large-scale fluctuations in the ionising radiation intensity and the gas temperature-density relation on the observable redshift space Ly α power spectrum. There are two independent effects on the power spectrum. The first arises from the clustering of sources and absorbers of radiation, which are assumed to trace the large-scale mass density fluctuations, each with their own bias factor. This clustering term is independent of the luminosity function, variability and anisotropic emission of the sources, as well as the size or other geometric properties of the absorbers: it depends only on how the density of sources and absorbers follow the underlying large-scale structure. The second effect is due to the fluctuations in the radiation intensity that arises from shot noise in the number of sources. This second term is independent of the source clustering, but depends on other source characteristics like the luminosity function. An analytical framework to treat these contributions to the Ly α power spectrum is described in section 2, and results for simple illustrating models are presented in section 3, with a discussion and conclusions in section 4. We use a Cold Dark matter cosmological model with parameter values that are consistent with the Planck collaboration (2013): $H_0 = 67.3$

km s $^{-1}$ Mpc $^{-1}$, baryon density $\Omega_b h^2 = 0.02205$, $\Omega_m = 0.315$, $n_s = 0.96$ and $\sigma_8 = 0.856$.

As this paper was being finalized, we became aware of the work by Pontzen (2014), presenting very similar ideas as here. We mention in section 4 the similarities and differences between the two papers.

2 ANALYTIC FORMALISM

The use of the Ly α forest as a tracer of large-scale structure lies on the principle that, when averaged over a large scale, the mean value of the transmission fluctuation through the Ly α forest, $\delta_\alpha = F/\bar{F}(z) - 1$ (where F is equal to the observed flux divided by a model quasar continuum, and \bar{F} is the mean value of F over all the universe at redshift z), has a linear relation to the local deformation tensor of large-scale structure when smoothed in the same way over a large scale. On small scales, the distribution of δ_α and its correlations have a complex dependence on the physics of non-linear collapse of the intergalactic gas into filaments and halos, and the shock-heating, ionisation and cooling of the gas. However, on large scales all these effects are absorbed into a first order dependence of δ_α on the local deformation tensor in the linear regime (e.g., Kaiser 1987),

$$\frac{1}{H(z)} \frac{\partial v_i}{\partial x_j}, \quad (1)$$

where \mathbf{v} is the peculiar velocity smoothed over a large scale in the same way as F , x is the comoving coordinate, and $H(z)$ is the Hubble constant at redshift z . For an observer measuring F along a direction specified by a unit vector \mathbf{n} , there are two first-order scalars that can be obtained from the deformation tensor: its trace, $H^{-1} \partial v_i / \partial x_i = f(\Omega_m) \delta$, where $f(\Omega_m) = d \log D(a) / d \log a$ is the logarithmic derivative of the growth factor $D(a)$, and the peculiar velocity gradient along the line of sight, $\eta = n_i n_j (\partial v_i / \partial x_j) / H$. Therefore, the fluctuation in the Ly α transmission must be given to first order by a linear combination of δ and η , with two bias factors, $b_\delta = \partial \delta_\alpha / \partial \delta$ and $b_\eta = \partial \delta_\alpha / \partial \eta$, with numerical values that depend on redshift and on the small-scale physics of the intergalactic gas (McDonald et al. 2000, McDonald 2003, Slosar et al. 2009, Slosar et al. 2011). Whereas galaxy surveys require only one bias factor to relate galaxy density to mass density fluctuations, the Ly α forest requires two of them because of the non-linear transformation from the Ly α optical depth to the observed transmission fraction, which alters the dependence on the direction vector of the observation \mathbf{n} .

This dependence on δ and η is only valid, however, if one assumes that no other independent physical quantities that are correlated on large scales can affect the value of δ_α ; in particular, a

homogeneous ionising background intensity is assumed. The quantity that matters for determining the Ly α transmission is the photoionisation rate, $\Gamma(\mathbf{x})$, obtained from the integration over frequency of the background intensity times the cross section. Its fluctuation is $\delta_\Gamma(\mathbf{x}) = \Gamma(\mathbf{x})/\bar{\Gamma} - 1$. Including these large-scale variations of the photoionisation rate, the total Ly α transmission fluctuation smoothed over a large scale is

$$\delta_a(\mathbf{x}) = b_\delta \delta(\mathbf{x}) + b_\eta \eta(\mathbf{x}) + b_\Gamma \delta_\Gamma(\mathbf{x}) . \quad (2)$$

where b_Γ is now a third bias factor for the photoionisation rate. Therefore, the total Ly α correlation depends now not only on the correlations of δ and η (which are related to the primordial linear power spectrum with redshift distortions), but also on the correlation of δ_Γ with itself, δ and η . We now compute these correlations, and we will do this taking into account two different effects: the fact that sources are clustered and trace the mass fluctuations, and the shot noise due to the random distribution of discrete sources.

2.1 Source Clustering

We assume that the sources of the ionising background have a spatial distribution tracing the mass density field, with a bias factor b_s , so the mean large-scale overdensity of sources is $\delta_s = b_s \delta$. In addition, the ionising radiation is being absorbed by a population of absorbers, which are Lyman limit systems as well as absorption systems with Lyman continuum optical depths below unity that have a comparable contribution to the overall absorption. This population of absorbers has a large-scale distribution that is affected by both the underlying mass density fluctuations and the radiation intensity fluctuations. So, the absorber density fluctuation can be written as $\delta_a = b_a \delta + b'_a \delta_\Gamma$. We expect these absorbers to increase in high density regions and decrease in response to an increased ionising intensity, so b_a should be positive and b'_a should be negative.

Even though the opacity to ionising photons depends on frequency, and a detailed treatment has to include the intensity spectrum and the combined effect of absorption and redshift modifying the background spectrum compared to that emitted by the sources, here we shall treat the opacity as a single quantity, neglecting the effect of redshift. The opacity due to absorbers with density fluctuation δ_a is $\kappa(\mathbf{x}) = \kappa_0[1 + \delta_a(\mathbf{x})]$, where the average mean free path for an ionising photon is $\lambda_0 = \kappa_0^{-1}$. The radiation intensity fluctuation at a point \mathbf{x} due to the combination of all sources at any position $\mathbf{x} + \mathbf{r}$ is

$$\delta_\Gamma(\mathbf{x}) = \int d^3r \kappa_0 \frac{[1 + \delta_s(\mathbf{x} + \mathbf{r})]e^{-\tau(\mathbf{x}, \mathbf{r})} - e^{-\kappa_0 r}}{4\pi r^2} \quad (3)$$

where r is the modulus of the vector \mathbf{r} . Defining

also \mathbf{u}_r to be the unit vector in the direction \mathbf{r} , the optical depth from \mathbf{x} to $\mathbf{x} + \mathbf{r}$ is:

$$\begin{aligned} \tau(\mathbf{x}, \mathbf{r}) &= \int_0^r dy \kappa_0 [1 + \delta_a(\mathbf{x} + y\mathbf{u}_r)] \\ &= \kappa_0 r \left[1 + \int_0^r \frac{dy}{r} \delta_a(\mathbf{x} + y\mathbf{u}_r) \right] . \end{aligned} \quad (4)$$

Neglecting second order terms in δ_s and δ_a , equation (3) is simplified to

$$\begin{aligned} \delta_\Gamma(\mathbf{x}) &= \int \frac{d\mathbf{u}_r}{4\pi} \int_0^\infty dr \kappa_0 e^{-\kappa_0 r} \\ &\cdot \left[\delta_s(\mathbf{x} + r\mathbf{u}_r) - \kappa_0 \int_0^r dy \delta_a(\mathbf{x} + y\mathbf{u}_r) \right] . \end{aligned} \quad (5)$$

For the second term involving the absorbers, the order of the integrals over r and y can be inverted, and we find:

$$\begin{aligned} &\int_0^\infty dr \kappa_0^2 e^{-\kappa_0 r} \int_0^r dy \delta_a(\mathbf{x} + y\mathbf{u}_r) \\ &= \int_0^\infty dy \kappa_0^2 \delta_a(\mathbf{x} + y\mathbf{u}_r) \int_y^\infty dr e^{-\kappa_0 r} \\ &= \int_0^\infty dy \kappa_0 e^{-\kappa_0 y} \delta_a(\mathbf{x} + y\mathbf{u}_r) , \end{aligned} \quad (6)$$

and so finally, changing the name of the dummy variable y back to r , and reexpressing the integral in terms of the variable $\mathbf{x}' = \mathbf{x} + \mathbf{r}$,

$$\delta_\Gamma(\mathbf{x}) = \int \frac{d\mathbf{x}'}{4\pi r^2} [\delta_s(\mathbf{x}') - \delta_a(\mathbf{x}')] \kappa_0 e^{-\kappa_0 r} . \quad (7)$$

This result is easy to understand, because an absorber actually acts in the same way as a negative source in this linear regime.

We now replace $\delta_\Gamma(\mathbf{x})$ and $\delta_s(\mathbf{x}')$, $\delta_a(\mathbf{x}')$ in equation (7) by their Fourier transforms, invert the order of the integrals over \mathbf{k} and \mathbf{x}' , and do the integral over \mathbf{x}' , to find that the Fourier transforms are related by

$$\begin{aligned} \delta_\Gamma(\mathbf{k}) &= [\delta_s(\mathbf{k}) - \delta_a(\mathbf{k})] W\left(\frac{k}{\kappa_0}\right) \\ &= [(b_s - b_a)\delta(\mathbf{k}) - b'_a \delta_\Gamma(\mathbf{k})] W\left(\frac{k}{\kappa_0}\right) , \end{aligned} \quad (8)$$

where

$$W(s) = \int_0^\infty dx \frac{e^{-x} \sin(sx)}{sx} = \frac{\arctan(s)}{s} . \quad (9)$$

Writing now equation (2) in Fourier space, and suppressing dependences on k for brevity, the correlation of the Fourier modes of the Ly α transmission fluctuation is

$$\begin{aligned} \langle \delta_\alpha \delta_\alpha \rangle &= b_\delta^2 \langle \delta \delta \rangle + b_\eta^2 \langle \eta \eta \rangle + b_\Gamma^2 \langle \delta_\Gamma \delta_\Gamma \rangle \\ &+ 2b_\delta b_\eta \langle \delta \eta \rangle + 2b_\delta b_\Gamma \langle \delta \delta_\Gamma \rangle + 2b_\eta b_\Gamma \langle \eta \delta_\Gamma \rangle . \end{aligned} \quad (10)$$

Using the linear redshift distortion theory of Kaiser (1987), the Fourier modes of δ and η are related by $\eta = f(\Omega_m) \mu_k^2 \delta$, where $\mu_k \equiv \mathbf{n} \cdot \mathbf{k}/k$, and the power spectrum without including the radiation term δ_Γ can be written as usual in the form

$b_\delta^2(1 + \beta\mu_k^2)^2$, where the redshift distortion parameter is $\beta = f(\Omega_m)b_\eta/b_\delta$. When the radiation term is included and expressed as a function of δ using equation (8), we find that the total Ly α power spectrum is given by

$$P_\alpha(k, \mu_k) = P_L(k) b_\delta'^2(k) [1 + \beta'(k)\mu_k^2]^2, \quad (11)$$

where

$$b_\delta'(k) = b_\delta + b_\Gamma \frac{(b_s - b_a)W(k/\kappa_0)}{1 + b_a'W(k/\kappa_0)}, \quad (12)$$

and $\beta'(k) = b_\delta\beta/b_\delta'(k) = b_\eta f(\Omega_m)/b_\delta'(k)$.

Therefore, the effect of the photoionisation rate fluctuations that is induced by the clustering of sources and absorbers is to modify the bias factor and redshift distortion parameter in the power spectrum, replacing them with the effective values b_δ' and β' that are scale dependent, while their product $b_\delta'\beta' = b_\delta\beta$ remains fixed. At small scales, W is very small and the bias factor has its usual value $b_\delta' = b_\delta$. But in the limit of large scales, W approaches unity and b_δ' reaches the asymptotic value of $b_\delta + b_\Gamma(b_s - b_a)/(1 + b_a')$.

We now interpret physically the variation of the effective bias b_δ' with the Fourier scale k . We mention first that any realistic model for the absorbers needs to have $0 > b_a' > -1$: the density of absorbers (which we identify with the observed population of Lyman limit systems, as well as lower column density systems that also contribute to the global absorption of ionising photons) needs to decrease with δ_Γ as the increased photoionisation reduces the size of the absorbing regions, but the relative fluctuation in absorbers cannot be reduced faster than that in the ionising intensity because this would imply a runaway unstable process where any slight increase in emission leads to an arbitrarily large increase in the mean free path and the ionising intensity as the absorbers are completely ionised. Moreover, the sign of b_δ is negative while that of b_Γ is positive, so if $b_s > b_a$, the effective bias factor b_δ' decreases in absolute value with scale. The simple interpretation is that on scales large compared to the mean free path of ionising photons, denser regions also have a greater ionising intensity, and so the corresponding increase of Ly α absorption that is caused by the higher density is reduced. If $b_\Gamma(b_s - b_a)/(1 + b_a')$ is larger than $-b_\delta$, then the value of b_δ' is actually positive in the limit of large scales. Ignoring for now the effect of the peculiar velocity gradient (we return to this in section 3), this means that the effect of the higher ionising intensity overwhelms that of the higher mass density, causing denser regions to have an increased Ly α transmission (or reduced absorption), opposite to the behavior on small scales. In this case, there needs to be a critical scale k_r where b_δ' has a root, and the only surviving term for the power spectrum in equation (11) is $P_\alpha(k_r) = P_L(k_r)(b_\delta\beta\mu_k^2)^2$. In practice, the power spectrum near $\mu_k = 0$ can never quite go

down to zero owing to the shot noise from individual sources of radiation, as discussed below, as well as non-linear effects from small scales which we are not including here, but a change of sign of b_δ' as a function of scale still implies the presence of a dip in the power spectrum at small μ_k which should be measurable in the observations.

2.2 Shot noise from individual sources

Our treatment so far includes only the correlation of sources and absorbers with the matter density fluctuations. Next, we consider the term that is added to the correlation function because of the shot noise from individual sources. We assume that all the ionising sources emit their radiation isotropically at a constant luminosity. As we shall discuss below, this assumption is crucial for our computation of the shot noise term, even though it does not affect the source clustering term calculated above. We start defining the source luminosity function, per unit of volume, as $\Phi(L)$. The mean emissivity of the ionising sources is

$$\epsilon_q = \int_0^\infty dL \Phi(L) L. \quad (13)$$

If all the sources have the same luminosity, the power spectrum of the relative emissivity fluctuations is simply equal to the inverse of the source density, $1/n_s = L/\epsilon_q$. With a distribution of luminosities, the fraction of the emissivity provided by sources of luminosity L is $L\Phi(L) dL/\epsilon_q$, and therefore the overall power spectrum is equal to the constant

$$4\pi C = \int_0^\infty dL \frac{\Phi(L)L^2}{\epsilon_q^2}, \quad (14)$$

where we have introduced the factor 4π in the definition of C for later convenience. The intensity correlation can now be obtained by multiplying by the kernel in equation (9), and applying the Fourier transform. It is also instructive, however, to directly compute the correlation function by considering the correlated intensity at two spatial positions separated by a distance x caused by the flux that arrives at the two points from the same individual sources.

We choose one of the two spatial positions to be at the origin of coordinates, $\mathbf{r} = 0$, and the other one to lie on the x-axis at a distance x . The ionising intensity fluctuation at the origin is

$$\delta_\Gamma(\mathbf{r} = 0) = \sum_i \frac{L_i}{4\pi r_i^2} \frac{\kappa_0 e^{-\kappa_0 r_i}}{\epsilon_q} - 1, \quad (15)$$

where the sum is over each source i located at a distance r_i from the origin. The intensity fluctuation at \mathbf{x} is similarly expressed, replacing r_i by $|\mathbf{r}_i - \mathbf{x}|$. Using the fact that the probability per unit of volume to find a source of luminosity L within dL at any point \mathbf{r}_i is $\Phi(L) dL$, the correlation function of

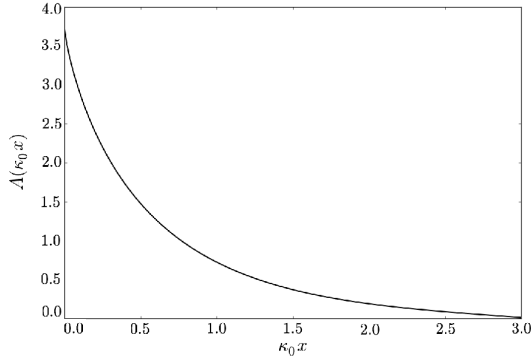


Figure 1. The dimensionless function A defined in equation (19), giving the shape of the intensity correlation function due to a set of randomly distributed, isotropic and constant sources of radiation.

δ_Γ is then obtained as

$$\xi_\Gamma(x) = \langle \delta_\Gamma(\mathbf{r} = 0) \delta_\Gamma(\mathbf{x}) \rangle = \quad (16)$$

$$\frac{C}{4\pi} \int d^3r \frac{\kappa_0^2 e^{-\kappa_0(r+|\mathbf{r}-\mathbf{x}|)}}{r^2 |\mathbf{r}-\mathbf{x}|^2}.$$

We compute this integral by transforming \mathbf{r} to spherical coordinates. Defining $\mu = \mathbf{r} \cdot \mathbf{u}_x / r$, where \mathbf{u}_x is the unit vector along the x-axis, and changing r to the variable $s = r/x$, the result is

$$\xi_\Gamma(x) = C \kappa_0^2 \int_0^\infty \frac{ds}{s} \quad (17)$$

$$\int_{-1}^1 d\mu \frac{\exp \left[-\kappa_0 x \left(s + \sqrt{1 + s^2 - 2s\mu} \right) \right]}{1 + s^2 - 2s\mu}.$$

This can be further reexpressed in terms of the exponential integral function, $E_i(x) = -\int_{-x}^\infty dt e^{-t}/t$. The final expression for the intensity correlation function is

$$\xi_\Gamma(x) = \frac{C \kappa_0^2}{x} A(\kappa_0 x), \quad (18)$$

where the dimensionless function A is (replacing $\kappa_0 x = \tau$ and $\kappa_0 r = \rho$)

$$A(\tau) = \int_0^\infty d\rho \frac{e^{-\rho}}{\rho} \quad (19)$$

$$\left[E_i \left(-\rho \sqrt{1 + \frac{\tau^2}{\rho^2}} \right) - E_i \left(-\rho \left| 1 - \frac{\tau}{\rho} \right| \right) \right].$$

The function A is plotted in Figure 1.

The sources that dominate the fluctuations in the ionising radiation intensity are the most luminous ones, which are well known from observations of the quasar luminosity function. We now estimate the constant C from recent measurements of the quasar luminosity function by (Ross et al. 2013), who used the BOSS survey of the SDSS-III Data Release 9 (see Eisenstein et al. 2011; Ahn et al. 2012; Dawson et al. 2013). The quasar luminosity function was fitted to a double power-law of the form,

$$\Phi_q(L) dL = \frac{\Phi_*/L_*}{(L/L_*)^{-\alpha} + (L/L_*)^{-\gamma}} dL. \quad (20)$$

The values of the fitted parameters obtained by Ross et al. (2013) are $\alpha = 1.52$, $\gamma = 3.10$, and $\Phi_*^{(R)} = 10^{-6.37} \text{ Mpc}^{-3} \text{ mag}^{-1}$, where they defined $\Phi_*^{(R)}$ to be a number density of quasars per unit of absolute magnitude. We convert their value $\Phi_*^{(R)}$ to our cosmological model, at $z = 2.25$ (the model used by Ross et al. 2013 had $\Omega_m = 0.30$ and $H_0 = 70 \text{ km s}^{-1} \text{ Mpc}^{-1}$) and to our units, finding $\Phi_* = 1.42 \times 10^{-6} (h^{-1} \text{ Mpc})^{-3}$. With these numbers, we compute the quantity C_q for quasars using equation (14), and we find $C_q = 9.5 \times 10^4 (h^{-1} \text{ Mpc})^3$. Note that the value of C_q is independent of L_* , and depends only on Φ_* and the shape of the luminosity function. The value of C_q diverges as γ approaches 3, so the fitted value of $\gamma = 3.1$ from Ross et al. (2013) implies a large uncertainty of C_q depending on the exact shape of the luminosity function at the high luminosity end.

The intensity of the ionising background is likely to have a contribution from galaxies, in addition to quasars. Assuming that all galaxies are much less luminous than the quasars that contribute appreciably to the constant C_q , then the faint galactic sources can increase the mean intensity, but can be neglected for the fluctuations, i.e., their contribution to the integral $\int dL \Phi(L) L^2$ is negligible. In that case, equation (14) implies that the emissivity power spectrum amplitude is determined by the constant

$$C = \frac{\epsilon_q^2 C_q}{(\epsilon_g + \epsilon_q)^2}, \quad (21)$$

where ϵ_g and ϵ_q are the emissivities of galaxies and quasars. The correlation due to shot noise is therefore reduced as the contribution from galaxies to the ionising intensity is increased.

Apart from the effect of galaxies, the amplitude of the intensity correlation function contributed by shot noise from the observed quasars that is obtained from equation (18) ought to be considered as an upper limit only. The reason is that real quasars are likely to emit anisotropically and to be highly variable in their luminosity on the light-crossing time of the cosmological scales at which the correlations are being measured. The effects of the variability and anisotropy of the emission from individual quasars can be highly complex and difficult to model, but an order-of-magnitude estimate can be made by assuming the opposite limit in which quasars emit in very narrow cones and short bursts. If f_Ω is the fraction of the solid angle over which the light of a quasar is emitted, and f_t is the fraction of time during which a quasar is shining, and we assume that the quasar luminosity is zero outside of this fraction of solid angle and time, then the correlation function ξ_Γ in equation (18) is reduced by a factor $f_\Omega f_t$, because assuming that a source is being observed at a point $\mathbf{r} = 0$, the probability that it is also observed at a point \mathbf{x} with the same luminosity is only $f_\Omega f_t$.

The total correlation function of the Ly α transmission is equal to the sum of the term due to source clustering, from equation (11), and the shot noise term in equation (18) multiplied by b_{Γ}^2 .

2.3 Values of the bias parameters

We now discuss how the values of the various bias parameters that have appeared in our derivation of the radiation effects in the Ly α correlation function can be estimated. All the bias factors should generally depend on redshift, and our discussion here will be focused at $z = 2.25$, the redshift near which the observations of Ly α correlations have so far been done with the BOSS survey.

We start with the bias factor that relates the ionising intensity fluctuations to the Ly α transmission fluctuations. As described in Font-Ribera et al. (2013) (see their equation 5.4), this bias factor can easily be calculated from its definition as $b_{\Gamma} = \partial\delta_{\alpha}/\partial\delta\Gamma$, where the values δ_{α} and δ_{Γ} are smoothed over sufficiently large, linear scales, if the true, unsmoothed distribution of the Ly α transmission is known, and under two additional assumptions: photoionisation equilibrium in a highly ionized medium (neglecting any contribution from collisional ionisation), and that any changes of temperature and hydrodynamic evolution of the intergalactic gas with the ionising background intensity can be neglected (in a more detailed treatment, small temperature variations would likely be induced by changes in the spectral shape of the ionising background rather than its intensity). In this case, the effect of the ionising intensity fluctuations is simply to divide the Ly α optical depth by a factor $1 + \delta_{\Gamma}$ at every pixel in the spectrum. If $P(F)$ is the unsmoothed probability distribution of F , one obtains

$$b_{\Gamma} = -\frac{1}{\bar{F}} \int_0^1 dF P(F) F \log(F). \quad (22)$$

At $z = 2.25$, the distribution of the Ly α optical depth, $\tau = -\log F$, can be approximated as a log-normal function, constrained to produce a mean transmission $\bar{F} = 0.8$ and a dispersion in the transmission $\sigma_F = 0.124$. This distribution yields a value $b_{\Gamma} \simeq 0.13$.

The values of b_{δ} and b_{η} have to be measured observationally. They are related to the redshift distortion parameter by $\beta = f(\Omega_m)b_{\eta}/b_{\delta}$ (Kaiser 1987). Measurements from the Ly α forest correlation in the scale range $10 - 60 h^{-1}$ Mpc in Slosar et al. (2011) resulted in a good measurement of $b_{\delta}(1 + \beta) = -0.336 \pm 0.012$ at $z = 2.25$, with a more poorly constrained $\beta \sim 1$. We shall assume $\beta = 1$, which is also favored by the measurement of cross-correlations (see Font-Ribera et al. 2012, 2013), and $b_{\delta} = -0.17$ (so $b_{\eta} = \beta b_{\delta}/f(\Omega_m) \simeq -0.17$; note that

the negative sign of b_{δ} and b_{η} results from the convention that δ_{α} is a transmission fluctuation, which is therefore negative when the mass density perturbation is positive). These observational results may change in the future since they were obtained by neglecting the radiation effects that are examined here, and they are subject to other possible systematic errors (e.g., Font-Ribera & Miralda-Escudé 2012).

For the bias of the sources, quasars have had their bias factor measured from their auto-correlation (White et al. 2012, and references therein) and cross-correlation with the Ly α forest (Font-Ribera et al. 2013), resulting in values in the range 3.5 to 4. The actual bias of the sources, however, depends also on the contribution that galaxies make to the ionising background intensity and on the bias factor of these galaxies. If the bias factors of quasars and galaxies are b_q and b_g , then $b_s = (\epsilon_q b_q + \epsilon_g b_g)/(\epsilon_q + \epsilon_g)$. Galaxies are on average associated with lower-mass halos than quasars, so their bias factor should be smaller and therefore b_s should be lower than b_q .

The population of absorbers determining the mean free path of the ionising radiation is dominated by systems that have an optical depth of order unity at the Lyman limit, with column densities $\sim 1.6 \cdot 10^{17} \text{cm}^{-2}$. Note that only systems with column densities above this value are usually referred to as Lyman limit systems, but absorbers of lower column density are about equally important (e.g., Miralda-Escudé & Ostriker 1990; Haardt & Madau 1996). The bias factor has only been measured for systems of higher column densities, the damped Ly α systems (Font-Ribera et al. 2012), and a value $b_a \simeq 2$ was obtained. Lyman limit systems are of lower column density than the damped systems but they should have a similar bias factor if halos of all masses give rise to the same distribution of hydrogen column densities, depending on the impact parameter. However, a population of low-mass halos might exist in which the self-shielded gas does not reach as high column densities as in high-mass halos, which would then reduce the mean bias factor of the Lyman limit systems. Both b_s and b_a are therefore rather uncertain. The effective Ly α forest bias depends only on the difference $b_s - b_a$ (see equation 12), for which we shall assume a fiducial value $b_s - b_a = 1$.

Finally, the bias factor controlling the response of the absorbers to changes in the ionising intensity can be related to the column density distribution of Lyman limit systems, which we model as a power-law, $f(N_{HI}) dN_{HI} \propto N_{HI}^{-a} dN_{HI}$. This implies a radial profile of the column density in spherical halos $N_{HI} \propto r^{2/(1-a)}$. In photoionisation equilibrium, the column density at a fixed radius r outside the region where the gas starts to self-shield will vary in proportion to the inverse of the pho-

toionisation rate. The self-shielding radius r_s occurs at a fixed column density, and will therefore change as $r_s \propto \Gamma^{(1-a)/2}$ in response to a change of the external ionising intensity. The cross section to produce a Lyman limit system scales as r_s^2 , so the number of absorbers that are intercepted per unit length should scale as Γ^{1-a} . For small changes in Γ this implies a bias factor $b'_a = 1 - a$. We shall use here $a = 5/3$ (the value corresponding to a gas density profile $\rho_g \propto r^{-2}$, and $N_{HI} \propto r^{-3}$), and therefore $b'_a = -2/3$.

With the values we adopt here for the fiducial model, the value of $b'_\delta(k)$ in equation (12) is plotted in the left panel of Figure 2, as the solid line. Here and in the rest of the paper, we use a mean free path $\lambda_0 = 300 h^{-1} \text{ Mpc}$ as our fiducial value. Observational estimates of the mean free path of an ionising photon for being absorbed by hydrogen in the intergalactic medium or Lyman limit systems give a value $\lambda_0 \simeq 350 h^{-1} \text{ Mpc}$ (Rudie et al. 2013). Our approximate treatment in section 2.2 neglects the redshift of the photons, which effectively acts in the same way as an additional source of opacity with a comoving mean free path of the order of the horizon, $c(1+z)/H(z) \simeq 3000 h^{-1} \text{ Mpc}$. The effective overall mean free path is therefore close to our fiducial value of $300 h^{-1} \text{ Mpc}$.

The two other curves in Figure 2 are for variations of the bias values that will be used in section 3. For our fiducial model, $b'_\delta(k)$ is positive in the limit of large scales and negative at small scales, and therefore changes sign at a critical scale k_r . Depending on the uncertain values of all the bias factors we have discussed, this critical scale can have very different values, and is likely to vary substantially with redshift.

2.4 Fluctuations due to helium reionisation

In addition to the intensity of the ionising background, the intergalactic medium may be affected by other physical elements that are correlated over large scales. Here we consider as another possibility the imprint that may have been left by helium reionisation in the temperature of the intergalactic gas. At the mean baryonic density of the universe, the recombination time at $z = 2.25$ is much longer than the age of the universe, and so is therefore the cooling time of photoionised gas. As helium is doubly ionised for the first time, probably by luminous quasars at $z \simeq 3$ (Worseck et al. 2011, and references therein), the gas is heated to a spatially variable temperature depending on the spectrum and luminosity of the sources producing the ionisation fronts that eventually overlap when reionisation ends (e.g., Miralda-Escudé & Rees 1994; McQuinn et al. 2009). The long cooling time then implies that the gas temperature at ev-

ery spatial location may keep a memory of the time at which helium reionisation occurred, or the spectral shape of the sources, or other characteristics that were imprinted at the reionisation time. If the temperature fluctuates according to $\delta T = b_T \delta \Gamma_e$, where $\delta \Gamma_e$ is an intensity fluctuation of the HeII-ionising radiation that was present at the reionisation time arising from sources that may long have been dead, then the observed Ly α transmission in hydrogen would vary as $\delta_\alpha = b_e \delta \Gamma_e$ owing to the dependence of the recombination coefficient on temperature, which follows the approximate relation $\alpha_{rec}(T) \propto T^{-0.7}$. Using similar arguments as in section 2.3 for deriving b_Γ , we can infer that $b_e = 0.7 b_\Gamma b_T$.

If the helium-ionising radiation intensity follows the same behavior as the radiation that ionised hydrogen, with a different mean opacity κ_{0e} , a similar derivation as in section 2.1 shows that the total power spectrum that includes also the clustering term for the sources inducing the helium-reionisation perturbations is the same as in equation (11), with the new bias factor

$$b'_\delta(k) = b_\delta + b_\Gamma \frac{(b_s - b_a)W(k/\kappa_0)}{1 + b'_a W(k/\kappa_0)} + b_e \frac{(b_{se} - b_{ae})W(k/\kappa_{0e})}{1 + b'_{ae} W(k/\kappa_{0e})}, \quad (23)$$

where the bias factors with the additional subscript e are the analogous ones for helium to those that were described for hydrogen in section 2.1.

3 RESULTS

The correlation function of δ_α is obtained from the Fourier transform of the power spectrum in equation (11), which includes the source clustering term. To include the shot noise term, the correlation ξ_Γ from equation (18) multiplied by b_Γ^2 must be added. Following the formalism and notation of Kirkby et al. (2013) (see their section 2.2), the multipole terms of the power spectrum of equation (11) have their usual form with the new scale-dependent bias factor $b'_\delta(k)$ and redshift distortion parameter $\beta'(k)$ (Kaiser 1987; Hamilton 1992):

$$P_{\ell,\alpha}(k) = P_L(k) b'^2_\delta(k) C_\ell[\beta'(k)], \quad (24)$$

where

$$C_0 = 1 + \frac{2}{3} \beta'(k) + \frac{1}{5} \beta'^2(k), \quad (25)$$

$$C_2 = \frac{4}{3} \beta'(k) + \frac{4}{7} \beta'^2(k),$$

$$C_4 = \frac{8}{35} \beta'^2(k). \quad (26)$$

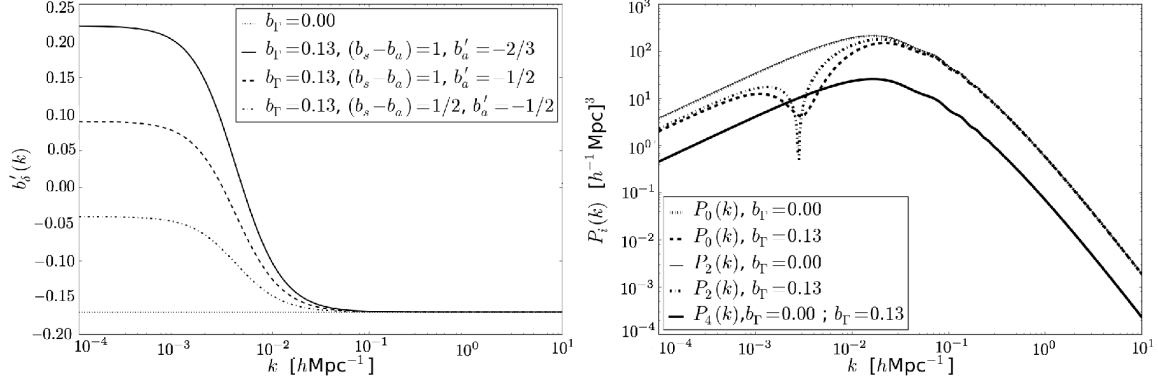


Figure 2. Effective bias (left) and power spectrum (right) of the Ly α forest, for several values of the bias parameters regulating the clustering strength of sources minus absorbers ($b_s - b_a$) and the response of the absorbers to the ionising intensity (b'_a). The dotted line is for no radiation effects, and the solid line in the left panel is for our fiducial radiation model. The mean free path is fixed to $\lambda_0 = 300 h^{-1} \text{Mpc}$. The right panel shows the monopole, quadrupole and hexadecapole of the power spectrum, for the cases of no radiation fluctuations and for our fiducial radiation model.

The multipoles of the real space Ly α correlation function are

$$\xi_\ell = \frac{i^\ell}{2\pi^2} \int_0^\infty dk k^2 j_\ell(kr) P_{\ell,\alpha}(k), \quad (27)$$

where j_ℓ are the spherical Bessel functions. Note that these correlation multipoles are no longer given by the equations in Hamilton (1992) because of the scale dependence of b'_δ and β' , except for the hexadecapole which does not change because $b'_\delta \beta' = b_\delta \beta$. We have used a Fast Fourier Transform method to calculate these multipoles numerically.

As shown in the left panel of Figure 2, the bias factor $b'_\delta(k)$ in our fiducial radiation model changes sign at a critical scale $k_r \simeq 0.005 h/\text{Mpc}$. The monopole, quadrupole and hexadecapole of the power spectrum are well defined and non-zero at $k = k_r$ because $b'_\delta \beta'$ is constant. At $k < k_r$, the redshift distortion parameter $\beta'(k)$ is negative. While the monopole is always positive for any value of β' , the quadrupole is zero when $\beta'(k) = -7/3$, and becomes negative at small k , when $-7/3 < \beta' < 0$. This is seen in the right panel of Figure 2, where the monopole, quadrupole and hexadecapole of the power spectrum are shown for the no radiation case, and the case that includes the source clustering effect for our fiducial values of the radiation bias parameters (the power spectrum is computed for the Cold Dark Matter model with the parameters mentioned in the introduction; all results for power spectra and correlation functions in this paper are shown at $z = 2.25$). The monopole has a dip near $k = k_r$, and the quadrupole has a root at the slightly smaller value of k where $\beta' = -7/3$. The reason for this behaviour is that when b'_δ is negative on large scales, high-density regions produce reduced absorption owing to the larger ionising intensity that overwhelms the gas density effect, but the gradient of peculiar velocity counteracts that, resulting in a negative quadrupole for the power spectrum.

The monopole and quadrupole terms in the Ly α correlation for our fiducial case of the values of the bias parameters discussed in section 2.3 are shown in the two panels of Figure 3, multiplied for convenience by x^2 . The dotted line is for a uniform ionising background. The well known Baryon Acoustic Oscillation peak appears at its characteristic scale of $\sim 100 h^{-1} \text{Mpc}$. The dashed, solid and dash-dot lines include the source clustering effect, with no shot noise, for three different values of the comoving mean free path: 200, 300 and $400 h^{-1} \text{Mpc}$ (our fiducial value used in all other figures is $\lambda_0 = 300 h^{-1} \text{Mpc}$). This mean free path decreases rapidly with redshift, which should change the way that intensity fluctuations modify the correlation function as the redshift increases.

The radiation from clustered sources adds a broadband term that is negative in the monopole and positive in the quadrupole. This is because the absolute value of the bias b'_δ in equation (12) is reduced at scales small compared to λ_0 , as long as $b_s > b_a$. The shorter the mean free path, the larger the radiation effects. On scales larger than the mean free path, the impact of the radiation on the monopole becomes positive. The effects are predicted to be relatively large, and they should be measurable as long as the broadband shape can be retrieved from the data without substantial systematic errors caused by the quasar continuum fitting operation. In the observations reported so far, broadband terms were marginalised over (Busca et al. 2013; Slosar et al. 2013; Font-Ribera et al. 2014) and therefore the effect of the ionising intensity fluctuations would not have been detected. Note that the position of the BAO peak is practically not affected; even if the peak shifts by a small amount owing to the addition of the radiation effects, any such shift should be further reduced when fitting with a parameterised broadband term.

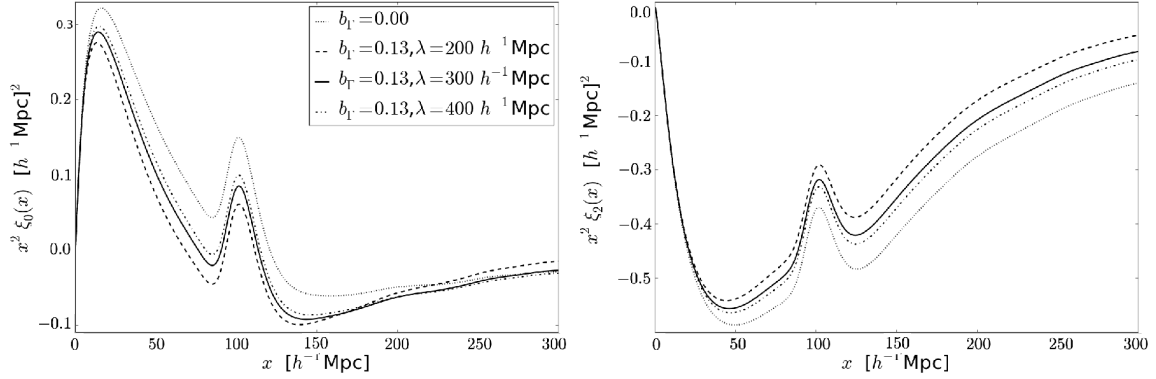


Figure 3. Monopole ($\ell = 0$, left) and quadrupole ($\ell = 2$, right) of the Ly α autocorrelation function. The dotted line is with no radiation effects, and the other three lines include them with our fiducial value of the bias factors in section 2.3 and three different values of the mean free path.

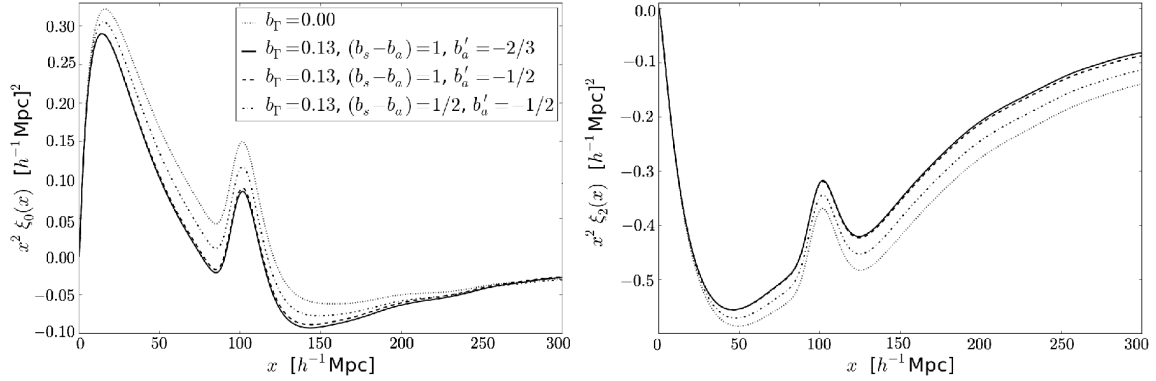


Figure 4. Monopole (left) and quadrupole (right) of the Ly α autocorrelation function, for different values of the bias parameters regulating the clustering strength of sources minus absorbers ($b_s - b_a$) and the response of the absorbers to the ionising intensity (b'_a). The dotted line is with no radiation effects. The mean free is fixed to $\lambda_0 = 300 h^{-1} \text{Mpc}$.

Figure 4 shows how the radiation effects vary with some of the bias parameters (again, with the monopole on the left panel and the quadrupole on the right panel). The dotted line (no radiation effects) and the solid line (for the fiducial values of the bias parameters in section 2.3) are the same as in Figure 3. The dashed line shows that the radiation effect is very insensitive to b'_a on scales small compared to λ_0 . The dash-dot line has a reduced value of $b_s - b_a$, and shows that the radiation effect is basically proportional to this bias difference between sources and absorbers.

Observations of the correlation function (or one-dimensional power spectrum) can also be done exclusively on the line of sight (McDonald et al. 2006; Palanque-Delabrouille et al. 2013). The correlation function along the line of sight is equal to the sum of all the multipoles. The result is shown in Figure 5 for some of the same models shown in Figures 3 and 4. This figure shows that the correlation along the line of sight on scales small compared to the mean free path is much less affected by the radiation fluctuations than the three-dimensional correlation.

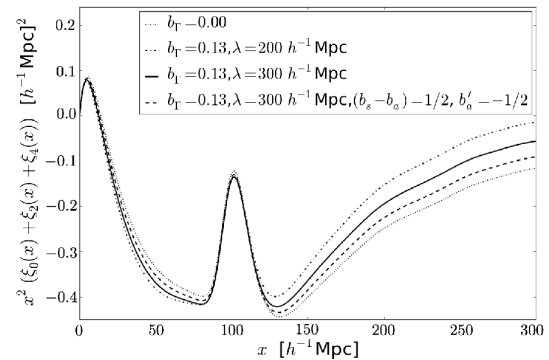


Figure 5. The sum of the monopole, quadrupole and hexadecapole of the Ly α autocorrelation function. The dotted and solid lines are as in Figures 2 and 3. The dash-dot line changes the mean free path to $200 h^{-1} \text{Mpc}$, and the dashed line shows the effect of changing the bias parameters from our fiducial model to the values indicated in the legend.

A simple model for the possible helium effect on the monopole of the correlation function, computed as explained in section 2.4, has been included

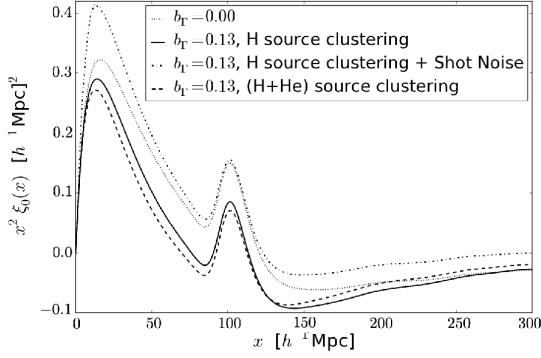


Figure 6. Monopole of the Ly α autocorrelation function. The dotted and solid lines are the same as in Figures 2 and 3. The dashed line includes the effect of helium reionisation, assuming an influence on the gas temperature with an effective mean free path $\lambda_{0e} = 30 h^{-1} \text{ Mpc}$. The dash-dot line shows the effect of adding the shot noise from individual sources, multiplied by a reduction factor as explained in the text.

in the dashed line in Figure 6. We have assumed a mean free path for the helium reionisation influence on the gas temperature of $\lambda_{0e} = \kappa_{0e}^{-1} = 30 h^{-1} \text{ Mpc}$, and a relation between the gas temperature fluctuation and helium-ionising intensity fluctuation of $b_T = 0.1$, implying $b_e = 0.0084$ (see section 2.4). The small value that we estimate for this bias factor means that the effect from the imprint on the gas temperature that may be left from double helium reionisation is very small, even with a much smaller mean free path than for the case of hydrogen. However, the effects might be more substantial if different spectra of the ionising sources in regions of different density gave rise to a larger variation of gas temperature than our assumed value $b_T = 0.1$.

The effect of shot noise is also analysed in Figure 6. The dotted and solid lines are again like in Figures 3 and 4 (only the monopole is shown here), and the dashed line adds to the solid one the shot noise term from equation (18), multiplied by b_T^2 , and multiplied also by a reduction factor that we now describe. If quasars are the sources of the ionising background with the luminosity function used in section 2.2, and they are isotropic and constant, the shot noise is an extremely large effect which brings the value of the correlation function near the BAO peak, at $x \simeq 100 h^{-1} \text{ Mpc}$, to $x^2 \xi_0(x) \simeq 2 (h^{-1} \text{ Mpc})^2$, well above the upper bound of the axis in Figure 6. However, as discussed at the end of section 2.2, the shot noise term is likely to be reduced by the contribution from galaxies to the ionising background (by the factor C/C_q in equation 21), the fraction of solid angle over which quasars emit their radiation, and the fraction of the time over which an individual quasar is emitting. For the purpose of visualisation, we multiply the shot noise by the overall factor

$$\frac{C}{C_q} f_{\Omega} f_t = \frac{1}{4} \frac{10 h^{-1} \text{ Mpc}}{\max(x, 10 h^{-1} \text{ Mpc})}. \quad (28)$$

The effect of variability in reducing the shot noise may reasonably be expected to scale as x^{-1} , because two points in the Ly α forest are affected by the same luminosity of a certain quasar only if they are both within the paraboloid of constant retarded time for the light emitted by the quasar that ionises the gas producing the observed Ly α absorption, and this paraboloid has a fixed width determined by the duration of the quasar luminous phase. We stress, however, that the effects of anisotropy and variability are complicated and that here we multiply the shot noise by this simple reduction factor for display purposes.

The result in Figure 6 shows that the shot noise can be a large and highly significant effect. Clearly, the case of constant and isotropic quasars was already ruled out by the observations of Slosar et al. (2011), which showed that the correlation function was well fitted by the linear approximation that generalises the redshift distortion effects (Kaiser 1987) to the Ly α forest. Even with a large reduction of the shot noise term, the effects are likely to be comparable to the source and absorber clustering term, and this will make the interpretation of any observed differences from linear theory to be complicated. One can hope, nevertheless, that by combining a detailed observation of the monopole and quadrupole terms, and using joint constraints from cross-correlations of the Ly α forest with quasars and other objects in addition to the Ly α autocorrelation, the impact of the biasing of sources and absorbers and the shot noise from a complex population of ionising sources can be disentangled in the future.

4 DISCUSSION AND CONCLUSIONS

The first observational determination of the large-scale Ly α power spectrum in redshift space by Slosar et al. (2011) showed a remarkably good agreement with the simple linear theory of redshift space distortions with the Cold Dark Matter power spectrum. The same conclusion was reached from measurements of the cross-correlations with damped Ly α systems and quasars (Font-Ribera et al. 2012, 2013). However, the ionising intensity fluctuations should have an impact on these correlations. We have presented an analytical framework in this paper to model these effects in the Ly α autocorrelation, which can also be easily generalised to the cross-correlation with quasars or other objects, assuming they contribute as sources of the ionising background. Our conclusion from the results obtained in a few illustrating cases is that both the clustering term that measures how sources and absorbers of the ionising background trace the mass density fluctuations, and the shot noise term that depends on the luminosity function and other properties of the sources, have an important and mea-

surable effect on the monopole and quadrupole of the Ly α autocorrelation. A substantial broadband term is added as a contamination to this autocorrelation, which is being marginalised over in present studies that are focused on inferring the scale of the Baryon Acoustic Oscillation peak (Busca et al. 2013; Slosar et al. 2013). As the modeling of the spectral calibration and quasar continua and the accuracy of the Ly α correlation measurements in BOSS and upcoming surveys improve in the future, we can look forward to a detection of the broadband terms induced by radiation fluctuations discussed in this paper.

There are several parameters that are important in determining how the Ly α correlation is modified by intensity fluctuations. These are the quantities appearing in equation (12) for the effective Ly α bias factor, and the mean free path of ionising photons. The additional shot noise term is also dependent on many characteristics of the sources: the luminosity function, luminosity history and emission anisotropy. Disentangling all these effects from a detailed measurement and model fit to the redshift-space autocorrelations and cross-correlations will probably be a difficult challenge. However, if the emission properties and typical luminosity histories of quasars can be well understood from an accurate determination of the quasar-Ly α cross-correlation, it should be possible to model the shot-noise contribution to the autocorrelation and to infer from the observations some constraints on the biasing terms that affect the source clustering term. It is also worth noting that in the Ly α power spectrum, the term proportional to μ_k^4 is affected by neither the source clustering nor shot noise effects, and the other two terms proportional to μ_k^2 and independent of μ_k can in principle be used to separate the influence of the source clustering and shot noise effects (the term proportional to μ_k^2 is not affected by shot noise for constant and isotropic sources, but would acquire a contribution for anisotropic and variable sources). The three-dimensional Ly α power spectrum therefore provides a way of separating the radiation influences by separating the multipole terms, which are predicted to have the specific features near the scale of the mean free path shown in Figure 2 can then be compared to constraints obtained from cross-correlations.

The conclusions of our work are in agreement with those of Pontzen (2014), who has presented very similar ideas with a somewhat different mathematical treatment. There are a few differences in the way that absorbers are treated, and our incorporation of the redshift distortion effects allows us to predict the different behavior of the monopole and quadrupole terms in the Ly α power spectrum, but the basic conclusions of the two papers are similar.

While the radiation intensity fluctuations make

the large-scale Ly α forest correlations substantially more difficult to interpret as a tracer of the primordial fluctuations in the universe, these complications practically do not affect the measurement of the Baryon Acoustic Oscillation scale, and they should constitute a new motivation for studying the evolution of the source and absorber population of the ionising background.

ACKNOWLEDGMENTS

SGG thanks the APC, especially the "Cosmology & Gravitation" group, for their hospitality during part of the time when this work was being carried out. We also thank David Kirkby, Pat McDonald and Andrew Pontzen for stimulating discussions and for sharing their work on this subject. This work is supported in part by Spanish grant AYA-2012-33938.

REFERENCES

- Ahn C. P., Alexandroff R., Allende Prieto C., et al. 2012, *ApJS*, 203, 21
- Becker G. D., & Bolton J. S. 2013, *MNRAS*, 245
- Busca N. G., et al. 2013, *A&A*, 552, A96
- Croft R. A. C. 2004, *ApJ*, 610, 642
- Croft R. A. C., Weinberg D. H., Katz N., & Hernquist L. 1998, *ApJ*, 495, 44
- Croft R. A. C., Weinberg D. H., Pettini M., Hernquist L., & Katz N. 1999, *ApJ*, 520, 1
- Croft R. A. C., Weinberg D. H., Bolte M., Burles S., Hernquist L., Katz N., Kirkman D., & Tytler D. 2002, *ApJ*, 581, 20
- Dawson K. S., Schlegel D. J., Ahn C. P., et al. 2013, *AJ*, 145, 10
- Delubac T., et al. 2014, submitted to *A&A* (arXiv:1404.1801).
- Eisenstein D. J., Weinberg D. H., Agol E., et al. 2011, *AJ*, 142, 72
- Font-Ribera A., & Miralda-Escudé J. 2012, *JCAP*, 7, 28
- Font-Ribera A., Miralda-Escudé J., Arnau E., et al. 2012, *JCAP*, 11, 59
- Font-Ribera A., Arnau E., Miralda-Escudé J., et al. 2013, *JCAP*, 5, 18
- Font-Ribera A., Kirkby D., Busca N. G., et al. 2014, submitted to *JCAP*, arXiv:1311.1767
- Haardt F., & Madau P. 1996, *ApJ*, 461, 20
- Hamilton A. J. S. 1992, *ApJ*, 385, L5
- Kaiser N. 1987, *MNRAS*, 227, 1
- Kirkby D. et al. 2013, *JCAP*, 3, 24
- Lee K.-G., Bailey S., Bartsch L. E., et al. 2013, *AJ*, 145, 69
- McDonald P. 2003, *ApJ*, 585, 34
- McDonald P., Seljak U., Cen R., Bode P., & Ostriker J. P. 2005, *MNRAS*, 360, 1471
- McDonald P., Seljak U., Burles S., et al. 2006, *ApJS*, 163, 80
- McDonald P., Miralda-Escudé J., Rauch M., et al. 2000, *ApJ*, 543, 1

- McQuinn M., Lidz A., Zaldarriaga M., et al. 2009, ApJ, 694, 842
- Meiksin, A., & White, M. 2004, MNRAS, 350, 1107
- Miralda-Escudé J., & Ostriker J. P. 1990, ApJ, 350, 1
- Miralda-Escudé J., & Rees M. J. 1994, MNRAS, 266, 343
- Nestor D. B. et al. 2013, ApJ, 765, 47
- Palanque-Delabrouille N. et al. 2013, A&A, 559, 85
- Planck collaboration 2013, arXiv:1303.5076v2
- Ross N. P. et al. 2013, ApJ, 773, 14
- Rudie G. C., Steidel C. C., Shapley A. E., Pettini M. 2013, ApJ, 769, 146
- Slosar A., Irsić V., Kirkby D., et al. 2013, JCAP, 4, 26
- Slosar A., Font-Ribera A., Pieri M. M., et al. 2011, JCAP, 9, 1
- Slosar A., Ho S., White M., Louis T. 2009, JCAP, 910, 19
- White M., Myers A. D., Ross N. P., et al. 2012, MNRAS, 424, 933
- White, M., Pope, A., Carlson, J., et al. 2010, ApJ, 713, 383
- Worseck G., Prochaska J. X., McQuinn M., et al. 2011, ApJ, 733, L24
- Zuo L. 1992, MNRAS, 258, 36